
Faculty of Engineering

Faculty Publications

This is a post-review version of the following article:

Minor Defect Correlation with Dynamic Elastic Properties of PFRC (polypropylene fiber-reinforced concrete)

Rishi Gupta, Adham El-Newihy and Mandeep Shah

2018

The final published version of this article can be found at:

<https://doi.org/10.1680/jemmr.15.00068>

Citation for this paper:

Gupta, R., El-Newihy, A., & Shah, M. (2018). Minor defect correlation with dynamic elastic properties of polypropylene fiber-reinforced concrete. *Emerging Materials Research*, 7(2), 109-117. <https://doi.org/10.1680/jemmr.15.00068>

Minor Defect Correlation with Dynamic Elastic Properties of PFRC

***Dr. Rishi Gupta**, Ph.D., P.Eng. FEC*

University of Victoria, Victoria, Canada, guptar@uvic.ca

Adham El-Newihy, MAsC

University of Victoria, Victoria, Canada

Mandeep Shah, MEng

University of Victoria, Victoria, Canada

*Rishi Gupta, Ph.D., P.Eng. FEC

Associate Professor, Department of Civil Engineering

University of Victoria, PO Box 1700

Stn CSC, ECS 314

Victoria, BC V8W 2Y2

guptar@uvic.ca, (250) 721-7033

Revision Date: September 12, 2017

Efficient rehabilitation of aging civil infrastructure requires innovative and emerging materials along with proper implementation of Structural Health Monitoring (SHM). Prior to identifying a strategic SHM technique understanding of defects in structures is vital. Common defects in concrete include consolidation problems and development of micro-cracks during consolidation or stress induction. Monitoring the dynamic characteristics of concrete can play an essential role in detecting real-time and early stages of deterioration. Much research is focused on detecting large defects, however not much information is available on detection of minor defects in composites like Fiber Reinforced Concrete (FRC). This study focuses on testing and monitoring concrete's dynamic elastic behavior using a non-destructive resonant frequency approach. The change of dynamic elastic properties of normal concrete under flexural and compression loading is analyzed. Moreover, an initial attempt to monitor the change of elastic behavior when Polypropylene fibers are added as reinforcement is also investigated. Experimental results show a decrease in the dynamic modulus of elasticity when minor defects are present and when polypropylene fibers are added to plain concrete mixture.

Introduction

When designing concrete structures, the modulus of elasticity is one of the significant properties required to relate stress and strain. Elastic deformation modulus is inherently applied to the linear portion of the loading cycle of concrete. The common stress-strain response of concrete can be described as linear when lower than 40% in stress and 1000μ in strain¹. Determining the static modulus of elasticity of concrete relies on the linear range of the stress-strain curve, however, the dynamic modulus of elasticity represents a more realistic property since it does not rely on destructive testing of concrete. Moreover, it is more appropriate to assess the dynamic modulus of elasticity in case of dynamically loaded structures since it captures the full cycle of loading and it relies fully on non-destructive approaches².

To extend the durability and life of concrete structures, reinforcement materials such as fibers are used. Using recycled synthetic fibers as reinforcement in structures has become a less expensive and more sustainable alternative for making concrete

more durable. Fiber use in concrete is primarily used to reduce micro-cracks forming from shrinkage and improving tensile strength thus improving durability. Synthetic fibers, such as Polypropylene fibers, are commonly used with concrete for their high tensile strength, low elastic modulus and non-corrosive performance providing greater toughness for with standing high impact strength and promote durability of concrete³. Polypropylene fibers are usually produced from melt spinning of polypropylene chips where a continuous monofilament is cooled through water quenching that are cut to specific lengths with a defined diameter. By interfering with the passive capillary microstructure of concrete, these fibers can decrease the possibility of plastic settlement from water evaporation. This changes the plastic behavior of concrete. Using Polypropylene Fiber Reinforced Concrete (PFRC) is thus suitable for structures subjected to environmental and service wear. Moreover, synthetic fibers alleviate dry and plastic shrinkage issues by bridging crack formation as concrete hardens. Quality improvement of concrete, when adding fibers, depends on the fiber type, aspect ratio, fiber treatment and geometry⁴. Studies on the addition of polypropylene fibers in concrete have shown that the

flexural strength of concrete and abrasion resistance increases and the workability and drying shrinkage decreases. However, the addition of synthetic fibers typically does not increase the compressive strength or the split tensile strength of concrete⁵. The volume fraction of fibers affects the composite strength. As the volume fraction increases, the composite strength linearly increases. Yet when mixed with a composite, different types of fibers give a different effect to the composite microstructure and sometimes may have an adverse effect on the strength⁶.

The development of cracks in concrete are divided into three stages. However, a common limitation is that micro-crack development at the early stages cannot be observed. Stage 1 includes micro-crack development at the micro scale which develops at the time at which loading is initiated. These micro-cracks begin to form at areas where pores and consolidation flaws exist within the composite and arise from shrinkage due to rapid water loss⁷. Stage 2 includes linking up of micro-cracks to produce finer cracks that are approximately 1 μ m to 50 μ m in width and length respectively⁸. Stage 3 includes the final macro-crack development where deformation localizes from a network of micro-crack. Crack formation reduces concrete durability, hence increasing the rate of reduction of elastic modulus.

Several studies investigated the relationship between the dynamic modulus of elasticity and static modulus of elasticity⁹. Factors such as the compressive strength, age and curing conditions were also considered when comparing dynamic properties of concrete. However, the change in structural integrity of concrete is not clearly compared with dynamic properties.

Usually, the dynamic modulus of elasticity is determined using non-destructive methods that relates to the dynamic wave response of an impulse. Since resonance is an inherent property of a structure, this study utilized using the resonant frequency to calculate the dynamic moduli in accordance with ASTM C215. In contrast, the impact resonant frequency method provides greater speed of testing and accepts specimens of different dimensions¹⁰. Dynamic modulus of elasticity (E_d), modulus of rigidity (G) and the dynamic Poisson's ratio (ν) can be calculated using the equations provided in ASTM C215. Several factors such as the specimen size, water to cement ratio, aggregate size and type are required to provide a closer estimation of the dynamic elastic modulus¹⁰.

Influence of Study

In this study, the dynamic modulus of elasticity is correlated to inherent material defects arising from common consolidation and curing operations. In addition, the effect of inherent cracks that can develop even when low level of loading is applied are also considered. These influences are denoted as "minor defects" due to their inherent size and lack of ability to easily detect them visually.

The purpose of this study is to use a resonant frequency based non-destructive approach to investigate early changes in dynamic mechanical properties of concrete under loading and due to preexisting defects. Moreover, the effect of adding synthetic polypropylene fibers to concrete of similar mixture proportions on resonant frequency is studied.

Experimental Program

To investigate the change in phase behavior of concrete, the experiment was divided into three concrete batches. Both Batch 1 and Batch 3 are comprised of a set of concrete prisms of size (100 \times 100 \times 350 mm) and cylinders of size (100 \times 200 mm). Batch 2 included a set of plain concrete prisms (150 \times 150 \times 530 mm) and cylinders (100 \times 200 mm in size). Both Batch 1 and Batch 2 are designated for studying the change in dynamic properties of normal (plain) concrete with minor defects designated as (NC1) for incremental induced cracks and (NC2) for honeycombed structures. Normal concrete mixture Batch 1 (NC1) was used in investigating the development of cracks under progressive loading in relation to the dynamic mechanical properties. Normal concrete mixture Batch 2 (NC2) investigates the changes in dynamic elastic properties when encountering a common consolidation error (surface honeycombing) of cast concrete. Batch 3 is designated for studying the dynamic properties of Polypropylene Fiber Reinforced Concrete (PFRC). Batch 3 is divided into three mixtures. A control mixture (NC3), a normal fiber content mixture (NFRC) and a high fiber content mixture (HFRC) will be compared to show the effect of increasing the volume fraction of fibers on the dynamic properties of FRC.

a) Materials

Ordinary Portland Cement Type 1 (OPC) and Class F fly ash were used as the common binder material between the mixtures. Coarse aggregates, with specific gravity of 2.7 and water absorption of 0.45%, and fine aggregate (crushed sand), with specific gravity of 2.6 and water absorption of 1.2% were used as aggregates for the mixtures. Two mixtures introduced in this study contain a percentage of fibers by total volume of the mixtures. Polypropylene macro-synthetic fibers, with an aspect ratio (l/d) of 50, are added with 0.6% and 1% by volume to produce NFRC) and HFRC respectively. Properties of the Polypropylene fibers are shown in Table 1. Fibers were added in the mix in accordance with ASTM C1116 Type III. An Alkyl Sulphate Air Entraining Agent (AEA) and Water Reducing Agent (WRA) were used as chemical admixtures in all batches for protecting the concrete in freeze-thaw cycles and allow easier workability respectively.

Table 1. Properties of Polypropylene Fibers

Mechanical Property	Unit	Amount
Fiber Length	mm	50
Specific Gravity	-	0.91
Aspect Ratio	%	0.5
Elastic Modulus	GPa	7.5
Tensile Strength	MPa	550
Water Absorption	%	0
Melting Point	°C	164
Thermal Conductivity	-	Low

b) Mixture Proportioning

For Batch 1 and Batch 2, the mixture design focused on regular strength concrete however, Batch 3 incorporated two different fiber contents of 0.6% and 1% to study the effect on dynamic properties of normal and high fiber content respectively. The mixture proportions used in this study are shown in Table 2.

Table 2. Mixture Proportioning

Batch		1	2	3		
Concrete Type		NC1	NC2	NC3	NFRC	HFRC
Binder	Kg/m ³	345	345	345	345	345
<i>OPC</i>	Kg/m ³	276	276	276	276	276
<i>Fly Ash</i>	Kg/m ³	69	69	69	69	69
Sand	Kg/m ³	815	815	815	815	815
Aggregate	Kg/m ³	1055	1045	1055	1055	1055
Water	Kg/m ³	107	140	148	148	148
WRA	ml/m ³	1883	1225	1883	1883	2389
AEA	ml/m ³	123	123	123	123	123
Fiber	Kg/m ³	0	0	0	5.259	9.204
w/c	-	0.3	0.4	0.4	0.4	0.4

c) Sample Preparation

For Batch 1, plain concrete mixture was prepared as follows. Initially, sand and coarse aggregates were dry mixed to allow a consistent and homogenous blend of the aggregates. Water quantities per batch are divided into two equal volumes. The first set of water was plain water and the second include water with all admixtures. A total of 16 cylinders and 8 beams were cast. Similarly, for Batch 2, the mixing procedure is similar to that of Batch 1. A total of 3 cylinders and 6 beams were cast. For Batch 3, the control concrete mixture was as the normal concrete mixture for Batch 2. Fibers were gradually added in bundles during mixing to allow homogenous spreading of the fibers throughout the mixture. All samples were cured in a water bath set at 23±1°C and

prepared using a conventional drum mixer 50L in capacity. A total of 6 cylinders and 6 beams were cast for each fiber dosage.

d) Testing Parameters

To ensure reliable consistency in all the fresh concrete mixtures, the slump, air content and fresh batch temperatures are all taken in accordance with ASTM C143, ASTM C231 and ASTM C1064 respectively¹¹. Mechanical testing of hardened concrete was composed of compressive testing using a Forney compression testing machine with 3000kN capacity for cylinders. For flexure testing an MTS machine with 250kN capacity using third-point loading arrangement was used for Batch 1 prisms tested at 28 days from casting in accordance with ASTM C39 and C78 respectively¹¹.

e) Impact Resonant Frequency Testing

Determining the resonant frequency is one of the key elements in defining the dynamic elastic properties of concrete. Testing was established in accordance with ASTM C215. This standard relates principles of impact and forced resonant frequency measurement. It is instituted on measuring the fundamental transverse, longitudinal and torsional frequencies to define the transverse elastic modulus (E_{dt}), longitudinal dynamic elastic modulus (E_{dl}) and the modulus of rigidity (G) of concrete respectively. The resonant frequencies in this study were determined using the impact resonance method. ASTM C215 defines the equations required for the prementioned moduli using the concrete specimen mass, a dimensional correction factor and the frequency obtained from vibrating the according to the modes shown in Figure 1. Note that when calculating the transverse elastic modulus, a correction factor 'T' is required. This factor is selected from a table relating the specimen radius of gyration and length ratio (K/L) and a presumed Poisson's ratio. For this study, the assumed Poisson ratio is 0.17 while the T factor for (100×200 mm) cylinders, (100×100×350 mm) prisms and (100×100×350 mm) prisms are 1.02, 1.52 and 1.51 respectively. ASTM C215 notes that the Poisson's ratio for water saturated concrete may be higher than 0.17, yet an incremental increase of 0.03 in the Poisson ratio changes the T factor by increments of 0.1. The deviation between the Poisson ratio increments increase when the K/L ratio is above 0.10.

Primarily, a PCB accelerometer, with a pickup sensitivity of 10 mV/g, and frequency range of 5 – 60 kHz, is attached to the concrete surface using a pliable adhesive wax. Voltage input is collected using a 4-channel NI 6069 data acquisition system. After attaching the accelerometer and positioning the concrete samples to the required mode of testing, a standard ball tip hammer, weighing 110±2 grams, was used to strike the surface at precise locations on the samples being tested as shown in Figure 1. Nodal support of the specimens was established through neoprene bars 8×25×150 mm and positioned as shown in Figure 1. For analyzing the input waveform, a Fast Fourier Transform (FFT) matrix was

used to obtain an amplitude-frequency output from the amplitude-time vibrational wave. The acceleration time-domain input wave was digitized to 1024 samples at a sampling acquisition rate of 20 KHz. The spectral line spacing in the frequency-domain output wave was 19.5 Hz. These requirements are modeled in a VI program using NI LabVIEW. From the output frequency domain graph, the peak value verifies the natural resonant frequency according to the test mode. Any frequency results above 10% from the average frequency of three consecutive impacts were discarded and the test was repeated.

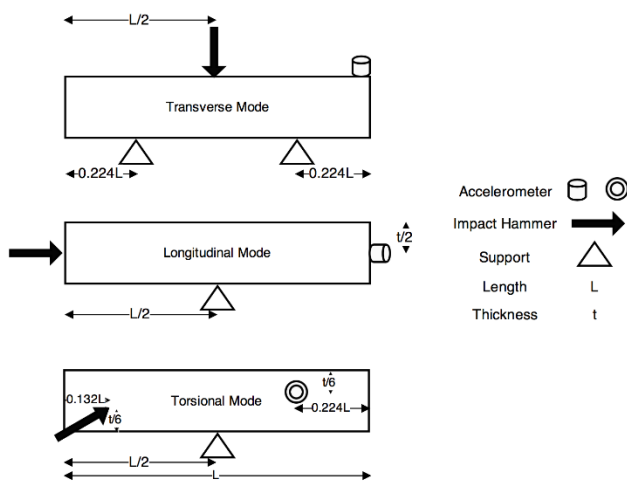


Figure 1. Transverse, longitudinal, and torsional setup adapted from ASTM C215¹²

Results and Discussion

a) Fresh Concrete Testing

Slump and air content values for all mixtures are shown in Table 3 and were within 110±30mm range. Using fibers in Batch 3 typically reduce the slump of concrete. Thus, the workability was adjusted by controlling the dosage of WRA to maintain a consistent slump range. The air content of all the mixes was between 3-7%.

Table 3. Fresh Concrete Properties

Batch	1		2		3	
	NC1	NC2	NC3	NFRC	HFRC	
Concrete Type	NC1	NC2	NC3	NFRC	HFRC	
Slump	mm	90	110	110	130	135
Air Content	%	3	6.3	6.8	4.2	4.6
Density	Kg/m ³	2500	2350	2518	2540	2479
Air Temperature	°C	8	15	6	6	6
Mixture Temperature	°C	9	16.5	5.3	5.5	5.2

b) Hardened Concrete Testing

Compressive strengths are relatively equal in Table 2 for all batches except Batch 1 where the w/c ratio was deliberately kept low to obtain a higher strength. This would enable studying mixtures with two different strengths (Batch 1 and Batch 2). Flexural strength of Batch 1 prisms average at 4.86 MPa. For Batch 3 prisms, addition of polypropylene fibers in NFRC and HFRC did not significantly change the compressive strength properties of control concrete NC3. However, flexural strength increased by 57% and 51% when using 0.6% and 1% of polypropylene fibers respectively.

Table 4. Hardened Concrete Properties

Batch	1		2		3	
	NC1	NC2	NC3	NFRC	HFRC	
Concrete Type	NC1	NC2	NC3	NFRC	HFRC	
Compressive Strength	MPa	50.1	30.1	33.2	32.6	30.3
Flexure Strength	MPa	4.86	-	4.32	6.79	6.51

c) Dynamic Testing

Resonant frequency was calculated for all specimens prior to any stress application according to ASTM C215 Impact Resonance Method. Specimens were then incrementally loaded 10-80% of the expected failure load both in compression and flexural modes. The expected failure load was determined by testing prototype specimens in both modes of loading. Batch 2 and Batch 3 were only used to study the influence of matrix strength when consolidation errors are determined and with the addition of polypropylene fibers respectively on the dynamic elastic moduli of normal-strength concrete. In Figure 1 and Figure 2, the frequency response ranges from 9 – 10 KHz and 5 – 6.5 KHz for the longitudinal and transverse frequency modes respectively.

Figure 2 shows the longitudinal and transverse frequency results for cylinders of Batch 1, Batch 2 and Batch 3. For Batch 1, at 10% of the ultimate compressive load, the transverse and longitudinal frequencies of the samples increased by 200 Hz. From 20 – 80% of the ultimate compressive load, the resonant frequency decreases constantly, as shown in Figure 1. The discussion that follows may not be clearly identifiable in Figure 1 due to the chosen scale. However, the scale selected in Figure 1 is intended to give a snapshot of the results for all specimens in a single figure. Both the longitudinal and transverse frequencies of NC1 cylinders show an increase in the resonant frequency when 10% of the compressive load is applied. This occurrence can relate to the closure of preexisting micro-cracks. These micro-cracks may have developed during early age of the concrete. When a compressive load is applied, the micro-cracks regress allowing the concrete to be condensed without plastically deforming. At this stage, the resonant frequency increases hence, the dynamic modulus of elasticity increases. The longitudinal and transverse resonant

frequencies decrease when 20% of the ultimate compressive load was applied. At this stage, the micro-cracks expand the network causing wider dislocations thus changing the microstructure². For Batch 2, the average resonant frequencies of defective cylinders are approximately 30% lower than that of normal cylinders. The specific details about the defects are discussed by the authors elsewhere¹². For Batch 3, a significant decrease in the longitudinal and transverse frequencies is shown, with a standard deviation of 0.5%, as the volume of fibers increases.

Figure 3 shows the longitudinal and transverse frequency results for prisms of Batch 1, Batch 2 and Batch 3. An average of 2.5% decrease, from frequency at no load, is shown for Batch 1. Conversely resonant frequency of Batch 1 beams decreased when 10% of the ultimate flexural load is applied. Batch 2 shows a substantial decrease when minor defects are present in the prisms¹². For Batch 3, a decrease in both the longitudinal and transverse resonant frequencies is shown when fibers are added however, the average transverse frequency of NFRC samples was higher than the control concrete mix. Note that some change in frequency is due to the difference in dimensions and weight of the specimens and is accounted for in the equations for calculating the dynamic modulus of elasticity.

Figure 4 shows the torsional frequency results for prisms of Batch 1, Batch 2 and Batch 3. Prism 2 is inconsistent with other prism results hence was removed from the dynamic moduli calculations. The torsional frequency presented about 40% of the transverse frequency and according to Popovics et al⁹ is reasonable. For scenario 1, the average dynamic modulus of rigidity (G) decreases by 2 GPa from 0 – 20%. A constant decrease in frequency with 20 – 40% of loading increase was observed. Table 5 shows the average and standard deviations of the dynamic moduli calculated in accordance with ASTM C215 with precision bias.

Next, the dynamic modulus of elasticity was calculated from the resonant frequencies. Figure 5 shows the dynamic modulus of elasticity results, calculated from the transverse frequency of cylinders, of Batch 1 and Batch 2. For Batch 2, the modulus of elasticity of defective cylinders are lower by approximately 10 GPa from Batch 2 normal cylinder however, standard deviation of defective cylinder results is 3.2%¹². Batch 3 dynamic modulus calculations show an apparent decrease between the control concrete NC3, NFRC, and HFRC samples. A decrease of 1 GPa is noted between NFRC and HFRC. This can be considered a slight decrease due to the presence of the change of 0.4% volume of fibers in NFRC and HFRC. Still the impact resonance method was able to capture this slight difference.

Figure 6 shows the dynamic modulus of elasticity results, calculated from the longitudinal frequency of cylinders of Batch 1, Batch 2 and Batch 3. Similar to the transverse elastic moduli of cylinder, Batch 1 shows an increase at 10% of the compressive load. Batch 2 shows a decrease of dynamic elastic moduli when consolidation defects are present¹². Batch 3 shows a decrease in the longitudinal dynamic modulus of elasticity when polypropylene fiber percentage increases.

Figure 7 shows the dynamic modulus of elasticity and dynamic modulus of rigidity results, calculated from the transverse and torsional frequency of prisms respectively, of Batch 1, Batch 2 and Batch 3. For Batch 1, a decrease in elasticity is noticed when between 0 – 20% of the ultimate flexural load is applied and elasticity remains constant beyond 20%. The modulus of rigidity for Batch 1 similarly shows the same pattern. For Batch 2, minor defects¹² show a significant decrease from normal concrete prisms. Batch 3 shows a constant decrease in transverse dynamic modulus of elasticity as fiber volume percentage increases. A decrease of approximately 2 GPa is shown between the NC3, NFRC and HFRC prisms. Some disagreement appears to occur because fibers are known to reduce crack propagation, however, poor positioning of fibers can pave a crack network reducing the composite strength¹³. For batch 3, as fiber content increases from 0 – 1%, the moduli of elasticity and rigidity decreases. This confirms with dynamic elastic modulus tests performed on polypropylene fibers using ultrasonic pulse velocities¹⁴. On the other hand, with metallic steel fiber additions, the modulus of elasticity is expected to increase since steel elastic modulus is higher than that of concrete¹⁵.

Figure 8 shows the dynamic modulus of elasticity results, calculated from the longitudinal frequency of prisms of Batch 1, Batch 2 and Batch 3. The average longitudinal modulus of elasticity is higher by approximately 2 GPa than the average transverse resonant frequency for all batches. For Batch 1, the shift of the dynamic modulus of elasticity is noticed when between 0 – 20% of the ultimate flexural load is applied. For Batch 2, the defect prisms are lower in elastic modulus than the normal prisms¹². Batch 3 prisms show a significant decrease in dynamic modulus with polypropylene fiber addition. The concrete static elastic modulus is highly sensitive to cracking and thus, the dynamic modulus of elasticity is affected¹⁰.

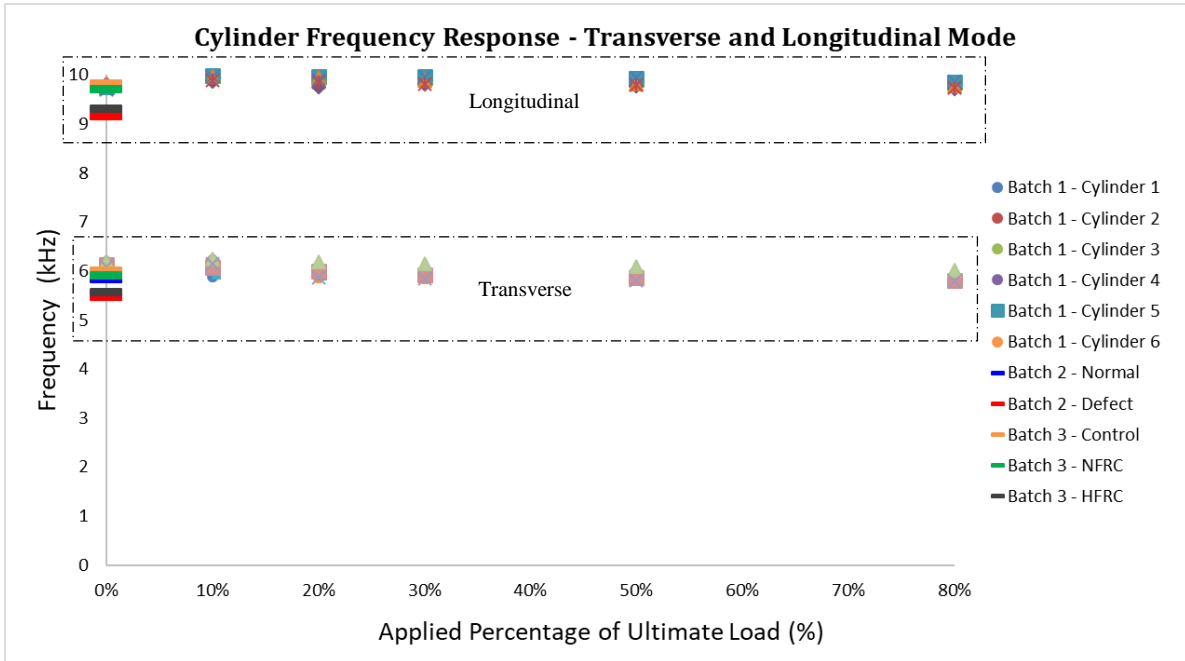


Figure 2. Cylinder Frequency Response – Transverse and Longitudinal Modes

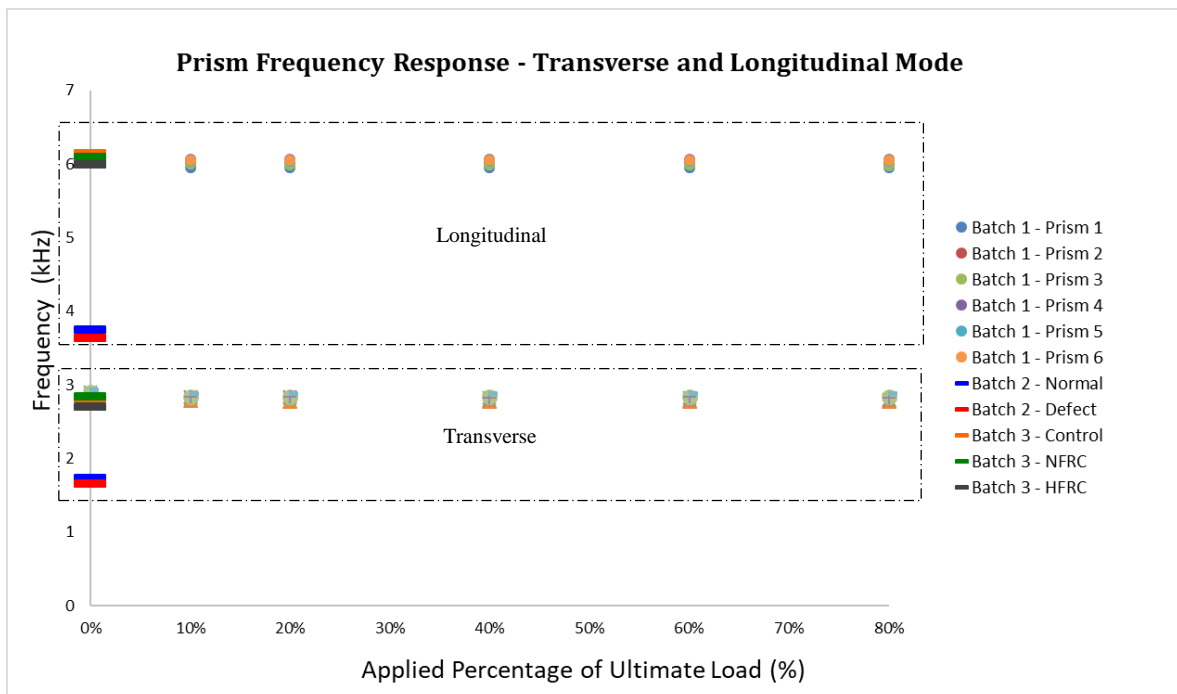


Figure 3. Prism Frequency Response – Transverse and Longitudinal Modes

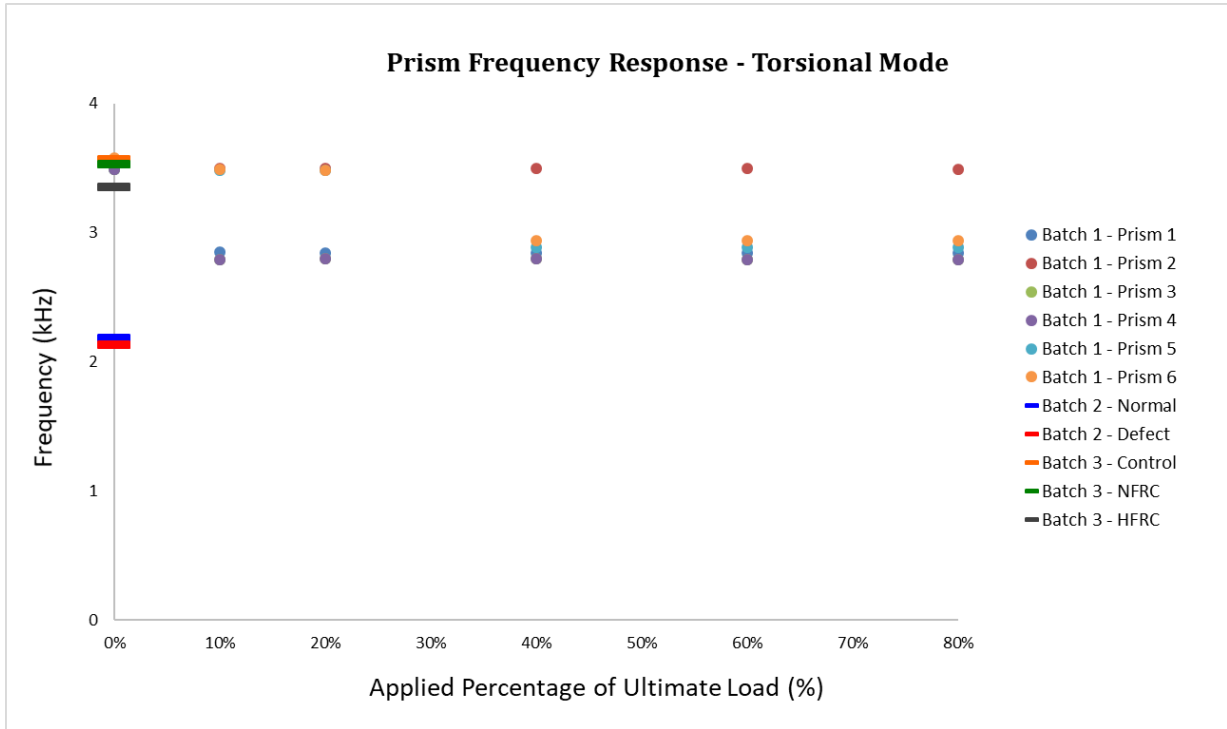


Figure 4. Prism Frequency Response – Torsional Mode

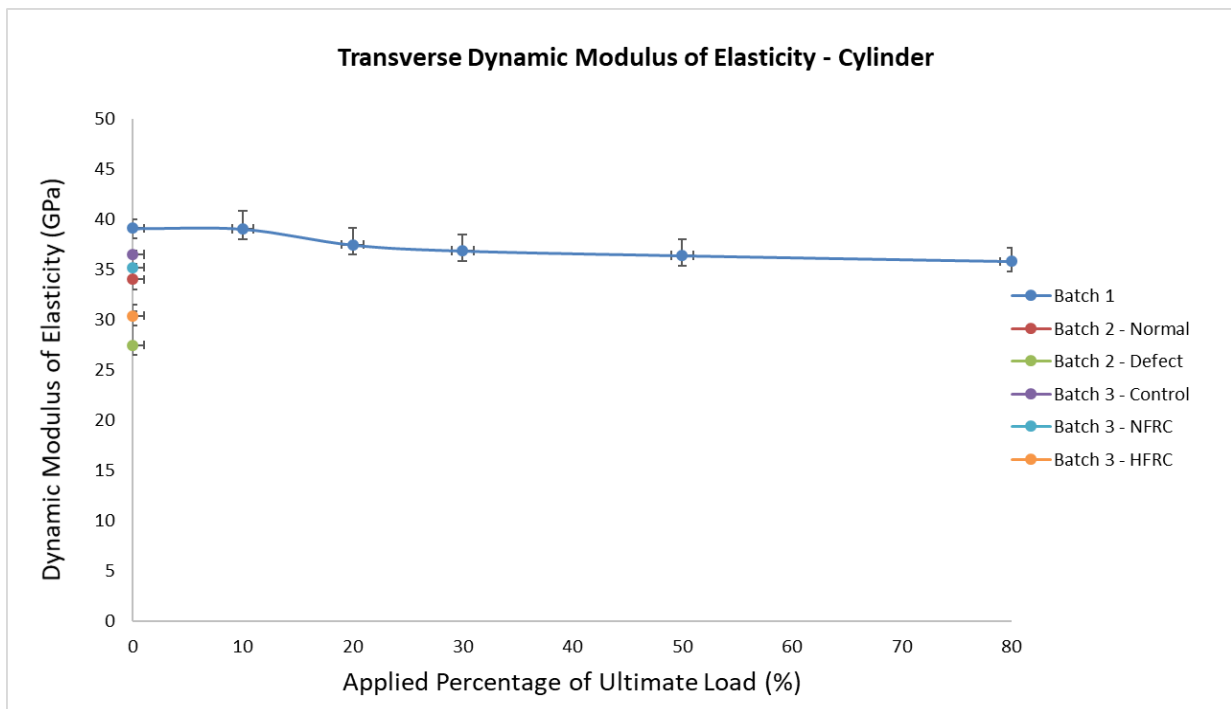


Figure 5. Cylinder - Transverse Dynamic Modulus of Elasticity

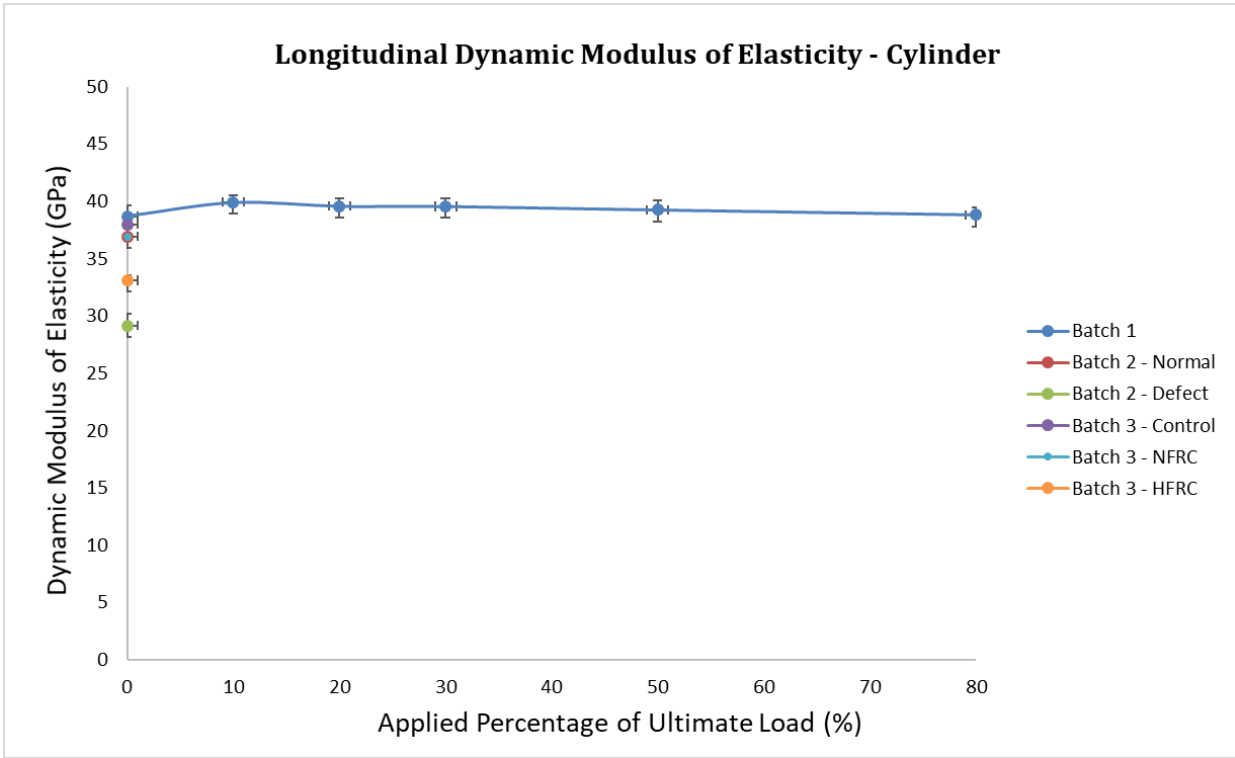


Figure 6. Cylinder - Longitudinal Dynamic Modulus of Elasticity

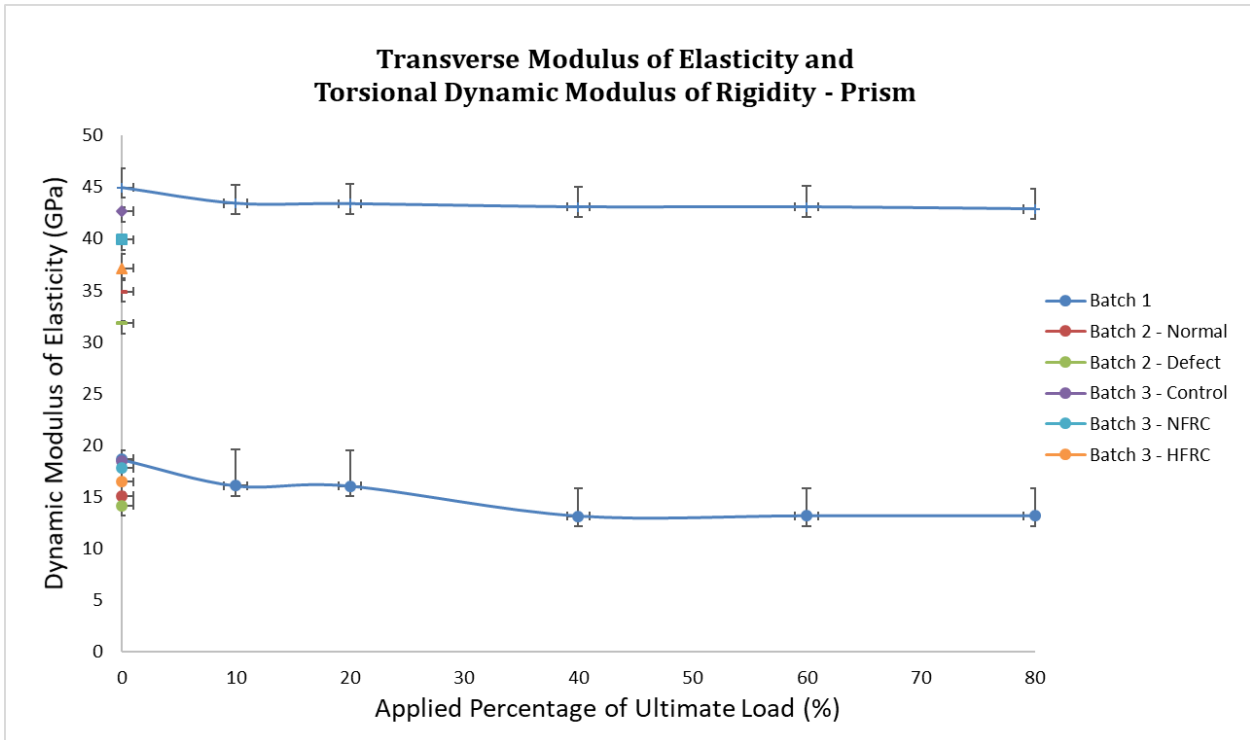


Figure 7. Prism - Transverse Dynamic Modulus of Elasticity and Torsional Dynamic Modulus of Rigidity

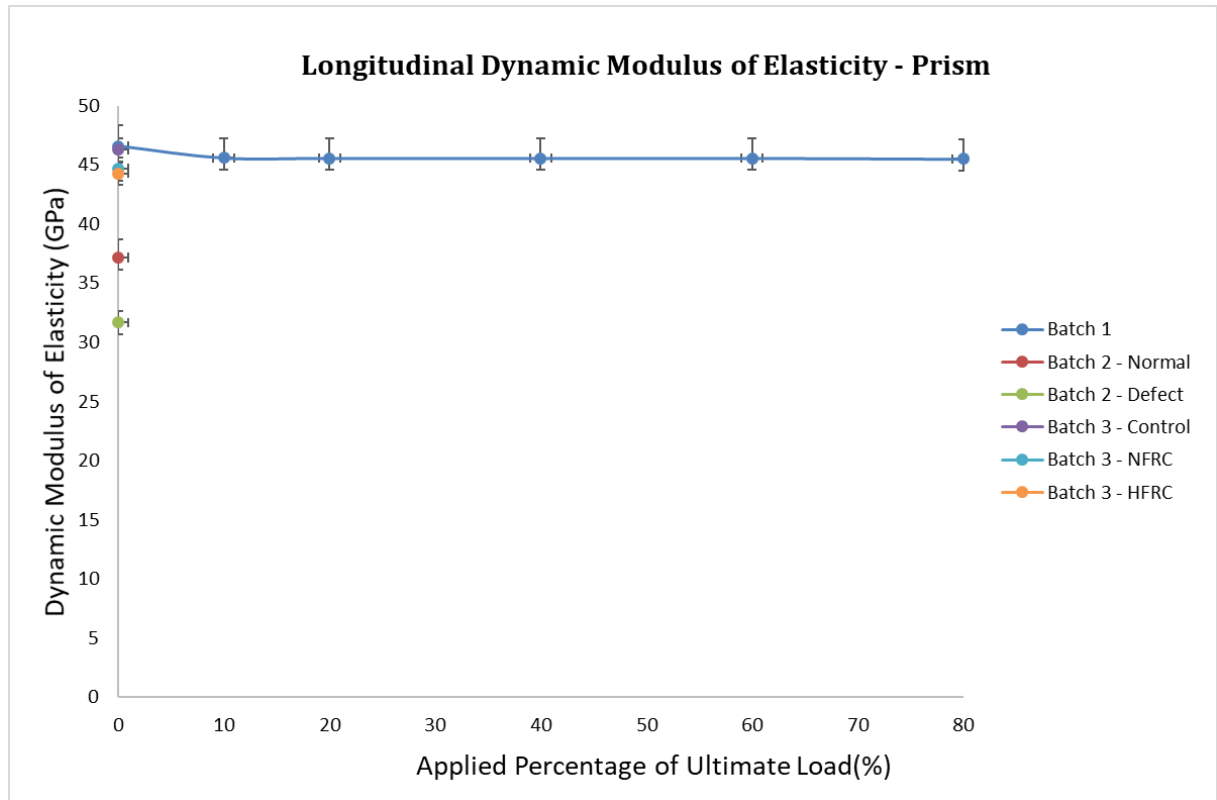


Figure 8. Prism - Longitudinal Dynamic Modulus of Elasticity

Cylinder	Type	Mean (GPa)			Standard Deviation (GPa)		
		Edt	Edl	G	Edt	Edl	G
Batch 1	Stress Induced	37.424	39.298	N/A	1.483	0.619	N/A
Batch 2	Normal	33.983	36.932	N/A	0.884	0.801	N/A
	Defect	27.441	29.149	N/A	3.993	3.141	N/A
Batch 3	Control	36.476	37.992	N/A	0.362	1.653	N/A
	0.6% PPF (NFRC)	35.181	36.924	N/A	0.303	1.304	N/A
	1% PPF (HFRC)	30.377	33.098	N/A	0.453	0.447	N/A
Prism	Type	Edt	Edl	G	Edt	Edl	G
Batch 1	Stress Induced	43.462	45.723	15.032	1.916	1.684	2.640
Batch 2	Normal	34.888	37.145	15.066	1.126	1.512	0.371
	Defect	31.791	31.666	14.157	0.235	1.126	0.120
Batch 3	Control	42.653	46.256	18.450	0.399	0.975	0.104
	0.6% PPF (NFRC)	39.913	44.673	17.761	0.532	1.559	0.417
	1% PPF (HFRC)	37.139	44.277	16.447	1.339	0.870	1.157

Edt: Dynamic modulus of Elasticity Transverse Mode (GPa)

Edl: Dynamic Modulus of Elasticity Longitudinal Mode (GPa)

G: Dynamic Modulus of Rigidity Torsional Mode (GPa)

PPF Polypropylene Fiber

Table 5 shows a summary of the dynamic elastic moduli of cylinders and prisms of batches 1, 2 and 3. Comparative baseline values of the moduli is shown at 0% loading. The standard deviation of all samples tested was between 0.12 and 3.993 GPa. However, it can be observed that defected concrete cylinders of batch 2 had a higher standard deviation as compared to the rest of the specimens. Authors hypothesize that this large deviation may be due to the change in density created from one end to the other end of the cylinder due to honey combing that results in non-uniform aggregate presence. However, it can be observed that if batch 2 defect cylinders are ignored, the standard deviation of all the specimens now would be between 0.235 to 1.916 GPa (not considering the modulus of rigidity) which correlates to a coefficient of variation range of 0.75% to 4.35% within in batch. These values are much smaller and hence within an acceptable error range indicating the viability of using this test method for detecting minor defects. It should be noted that if the coefficient of variation is calculated for resonant frequencies, these values are even smaller when compared to the values reported above for elastic moduli.

When the defect Batch 2 prisms are ignored, the calculated longitudinal elastic moduli in all specimens is higher than the corresponding transverse moduli. This can be attributed to the assumed value Poisson's ratio during calculation of the transverse moduli correction factor 'T'.

By adding polypropylene fibers in concrete for Batch 3, the average dynamic moduli decreased with increase of fiber volume from 0.6% to 1%. This shows that the fibers provide a more ductile matrix for the same concrete volume indicated through the decrease of the transverse and longitudinal elastic moduli when compared to the control specimens. Like Batch 1 and 2, the impact resonant frequency method can capture the slight change in moduli when the fiber volume increase by 0.4%.

The elastic moduli calculated using the resonant frequency method of cylinders is considered lower than that of the same calculated moduli of prisms. This may be attributed to the support conditions for cylinders that affect the natural vibration when opposed to vibrating the larger mass of prisms. Equations provided by ASTM C215 do not consider the true composite nature of concrete through cylinders hence; the dynamic modulus of elasticity calculated from cylinders may not have a true estimated value of the elastic modulus. Moreover, the longitudinal moduli of cylinders show an over estimation when compared to that of the transverse moduli. Correction factors using Love's equations¹⁶ can mitigate these inconsistencies yet were not used since only differences between mixtures are compared in this study. This confirms with the study by Popovics et al⁹ between the static and dynamic modulus of elasticity of concrete.

Conclusion

Dynamic elastic properties, such as the modulus of elasticity and modulus of rigidity of cracked or surface defected concrete can be determined by evaluating the resonant frequency. In this study, the dynamic modulus of elasticity is calculated for three concrete batches composed of cylinders and prisms tested in the transverse and longitudinal modes. Furthermore, the torsional frequency was measured to calculate the modulus of rigidity of concrete prisms.

The results show that the dynamic modulus of elasticity for concrete cylinders underestimates the value when compared to that of prisms with the same concrete formulation. Yet, testing the cylinders solely for observing the change in elastic properties when defects, such as cracks and surface honeycombing, along with the addition of synthetic fibers to concrete was clearly indicated through the attained frequency measured by impact resonance testing. It can be concluded that minor defects induced by loading specimens from 0 to 10% of the ultimate compressive and flexural load shows change in frequency for most specimens. Also, dynamic elastic moduli decreases with increase of polypropylene volume content in PFRC. Moreover, as the volume percentage of polypropylene fibers used in concrete increased, the natural resonant frequency decreased hence, the dynamic elastic moduli decreased proportionally while accounting for difference in mass and dimensions of the specimens. The resonant frequency method (conducted in accordance with to ASTM C215) has shown to be a reliable, cost effective and repeatable approach for detecting minor defects and compositional changes in concrete.

Future Work

Figure 2, Figure 5 and Figure 6 indicate an increase in the resonant frequency and dynamic elastic moduli when 10% of the ultimate load is applied in compression. This occurrence should be further studied as it may indicate the compression of concrete's microstructure without further crack propagation at this applied load. Moreover, dynamic testing on fiber reinforced concrete undergoing finer percentages along with incremental flexural loads should be further investigated.

Acknowledgment

The authors would like to acknowledge the polypropylene fibers donated by Propex Inc. and the financial support of NSERC.

References

1. Lamond J, Pielert J. Significance of tests and properties of concrete and concrete-making materials. Philadelphia, PA: ASTM; 2006.

-
2. Mindess S, Young J. Concrete. Englewood Cliffs, N.J.: Prentice-Hall; 1981.
 3. Naaman A, Wongtanakitcharoen T, Hauser G. Influence of Different Fibers on Plastic Shrinkage Cracking of Concrete. *ACI Materials Journal*. 2005;102(1):49-58.
 4. Banthia N, Gupta R. Influence of polypropylene fiber geometry on plastic shrinkage cracking in concrete. *Cement and Concrete Research*. 2006;36(7):1263-1267.
 5. Kakooei S, Akil H, Jamshidi M, Rouhi J. The effects of polypropylene fibers on the properties of reinforced concrete structures. *Construction and Building Materials*. 2012;27(1):73-77.
 6. Brahim S, Cheikh R. Influence of fibre orientation and volume fraction on the tensile properties of unidirectional Alfa-polyester composite. *Composites Science and Technology*. 2007;67(1):140-147.
 7. Neville A, Brooks J. Concrete technology. Harlow, Essex, UK: Longman Scientific & Technical; 1987.
 8. Lawler J, Wilhelm T, Zampini D, Shah S. Fracture processes of hybrid fiber-reinforced mortar. *Mat Struct*. 2003;36(3):197-208.
 9. Popovics J, Zemajtis J, Shkolnik I. A study of Static and Dynamic Modulus of Elasticity of Concrete. *ACI Structural Journal* [Internet]. 2008 [cited 8 January 2014]:ACI CRC. Available from: https://www.concreteresearchcouncil.org/portals/7/files/pdfs/crc_43.pdf
 10. Malhotra V, Carino N. Handbook on nondestructive testing of concrete. Boca Raton, Fla.: CRC Press; 2004.
 11. Annual Book of ASTM Standards. West Conshohocken; 2014.
 12. Gupta R, El-Newihy A. Effectiveness of resonance frequency based method to predict moduli of concrete and detection flaws. Nagasaki, Japan: JCI: International Conference on the Regeneration and Conservation of Concrete Structures; 2015.
 13. Deng Z, Li J. Mechanical behaviors of concrete combined with steel and synthetic macro-fibers. *Computers and Concrete*. 2007;4(3):207-220.
 14. Martinez-Barrera G, Urena-Nunez F, Gencel O, Brostow W. Mechanical properties of polypropylene-fiber reinforced concrete after gamma irradiation. *Composites Part A: Applied Science and Manufacturing*. 2011;42(5):567-572.
 15. Pawade P, Nagarnaik P, Pande A. Performance of steel fiber on standard strength concrete in compression. *International Journal Of Civil And Structural Engineering*. 2011;2(2):483 - 489.
 16. Love, A. (1944). A treatise on the mathematical theory of elasticity. New York: Dover Publications.